



A fast hybrid roundness evaluation algorithm based on computational geometry and particle swarm optimization for profiles with massive points

Xuelong Bai^{a,b}, Wei Wang^a, Wenhao li^{a,*}, Zhaowu Liu^a, Shuo Yu^a, Yu Bai^{a,b}, Guoxue Chen^{a,b}

^a Changchun Institute of Optics, Fine Mechanics and Physics, Chinese Academy of Sciences, Changchun 13033, China

^b University of Chinese Academy of Sciences, Beijing 100049, China

ARTICLE INFO

Keywords:

Roundness

Minimum zone circle

Computational geometry

Particle swarm optimization

ABSTRACT

The advancement of measurement has led to rigorous demands for the accuracy and efficiency of roundness evaluation of minimum zone circle (MZC) for profile with massive points. Existing algorithms struggle to balance efficiency and accuracy in such cases. A fast hybrid roundness evaluation (HCGPSO) algorithm for MZC based on the computational geometry (CG) and particle swarm optimization (PSO) algorithm is proposed, which incorporates a CG-based global best (gBest) selection method into the PSO algorithm and refines the termination criterion. A comparison with the published studies demonstrated that the HCGPSO algorithm were accurate and result are displayed to 10^{-15} mm. The impact of target accuracy, the harmonic and the number of points contained in profile on the performance of proposed algorithm are analyzed. With sub-nanometer target evaluation precision, HCGPSO enhances efficiency by an average of 64 % for profiles containing the highest harmonics from 30 undulations per revolution (upr) to 500 upr with 1500 points. For profiles with 300 to 4000 points at 150 upr, an average efficiency enhancement of 60 % was observed. For profiles with 4000 points at 500 upr from four workpieces, the calculation time is reduced by 55 % on average compared to the PSO algorithm, with increased accuracy and stability.

1. Introduction

Roundness can be used to evaluate the difference between a measured profile and standard circle, and is widely applied to evaluate the quality of a measured object in industry [1–3], machinery [4–6], and other fields [7,8] as shown in Fig. 1. Gyro is used in high-resolution satellites and space telescopes to accurately perceive motion postures [3], which places extremely high demands on the mechanical accuracy of rotating workpieces such as universal joints and rotors. Roll-to-roll manufacturing technology can be used to manufacture, for example, flexible electronic devices, functional films, paper, and fabrics. The mismatching of roller axes, roundness errors, and imbalances may cause runout and tension disturbances, which lead to reduced product quality [1]. For some high-end equipment, such as high-speed trains and tunnel-boring machines, the mechanical accuracy of bearings has a significant impact on equipment performance [6]. In the biological and chemical fields, roundness can be used to evaluate the quality of the printing droplets of bacterial arrays for biosensors [7]. The size and shape of Alginate-based hydrogels which used in drug delivery and cell encapsulation is also significant parameter [8].

It can be seen that rotary workpieces are evidently significant across various domains. With the continuous advancement of precision machining and measurement techniques, there is an increasingly requirement for the accuracy of roundness evaluation algorithms. The accuracy of the profile evaluation algorithm must be significantly higher than the measurement accuracy so that no additional errors are introduced during the evaluation stage. The uncertainty or accuracy requirements of some rotary standard parts that are often used for calibration of high-precision instruments have reached the nanometer level [9,10]. In the field of machine tool error calibration, nanometer or even sub-nanometer profile measurement accuracy has become very common with the application of high-precision capacitive sensors and error separation technology [10–13]. At the same time, the profile measurement accuracy of professional roundness/cylindricity measuring instruments has also reached nanometer accuracy or uncertainty [14,15]. With nanoscale profile measurements, the accuracy of the roundness evaluation algorithm must reach the sub-nanometer to effectively prevent the introduction of additional errors in the calculation stage. Furthermore, ultra-high-precision surface processing technology [16] and sub-nano displacement technology [17] are also being

* Corresponding author.

E-mail address: liwh@ciomp.ac.cn (W. li).

developed. Therefore, roundness error evaluation with sub-nanometer precision is imperative. To provide richer profile information and a more accurate quality evaluation [18,19]. More and more sampling points of profile are also required. In some cases, real-time parameter detection is also required [2]; hence, developing a fast and accurate roundness evaluation algorithm for a profile with massive points is of great importance.

ISO 12181-1 stipulates four roundness evaluation methods, that is, least squares circle (LSC) method, MZC method, minimum circumscribed circle (MCC) method, and maximum inscribed circle (MIC) method, of which the MZC method is the only method that complies with the definition of roundness, and roundness evaluated by the MZC method is minimum. When there is a dispute over the roundness of a workpiece, the MZC method should be applied to evaluate roundness [20].

At present, two main types of MZC evaluation algorithms exist; one is based on CG. The center of the MZC can be determined by four control points [21,22], which satisfies the 2 + 2 model of two control points C, D on the inner circle and two control points E, F on the outer circle. It can be seen that the exhaustion of the control points can identify MZC; however, the calculation required for an n -point dataset is $n!/4!(n-4)!$. An increase in the number of points leads to a rapid increase in computational complexity. Most recent research on roundness evaluation based on CG is devoted to find the accurate four control points efficiently [23-29], as shown in Table 1. Xiuming and Zhaoyao [25] introduced the convex hull to eliminate some redundant data in polar

coordinate and then calculate the roundness with the proposed minimum zone lines method. Calvo and Gomez [26] used the idea of calculating straightness to calculate the MZC, MIC and MCC in polar coordinates. Liu et al. [27] proposed an intersecting chord method to calculate MZC of the profile obtained from coordinate measuring machine (CMM). The method is based on the cross relationship between the chord constructed by the inner control points and the outer control points, rather than the calculation of search step and search direction, which effectively saves calculation time. Khilil et al. [28] proposed the alternative exchange method, which randomly selects three points and then designs an exchange criterion to update the last outer point to find the possible combinations of control points for the MZC. Zhuo et al. [29] summarized the angle relationship of the control points in the minimum zone criterion and designed a control point update method based on this relationship to calculate MZC. Such CG-based algorithms make complex provisions and calculations to determine the next iteration direction, and most of the algorithms are for profiles from a CMM that have fewer than 200 points.

The other type of MZC evaluation algorithm consists of nonlinear optimization algorithms. Owing to their flexibility, robustness, and versatility, nonlinear optimization algorithms find extensive application in various fields [30-37], such as high-dimensional optimization problems, image segmentation, traveling salesman problems, etc. They have also made progress in the field of MZC evaluation recently [38-46], as shown in Table 2. Sun [38] and Du et al. [39] used the PSO algorithm to evaluate the MZC and optimized the parameter selection of the PSO

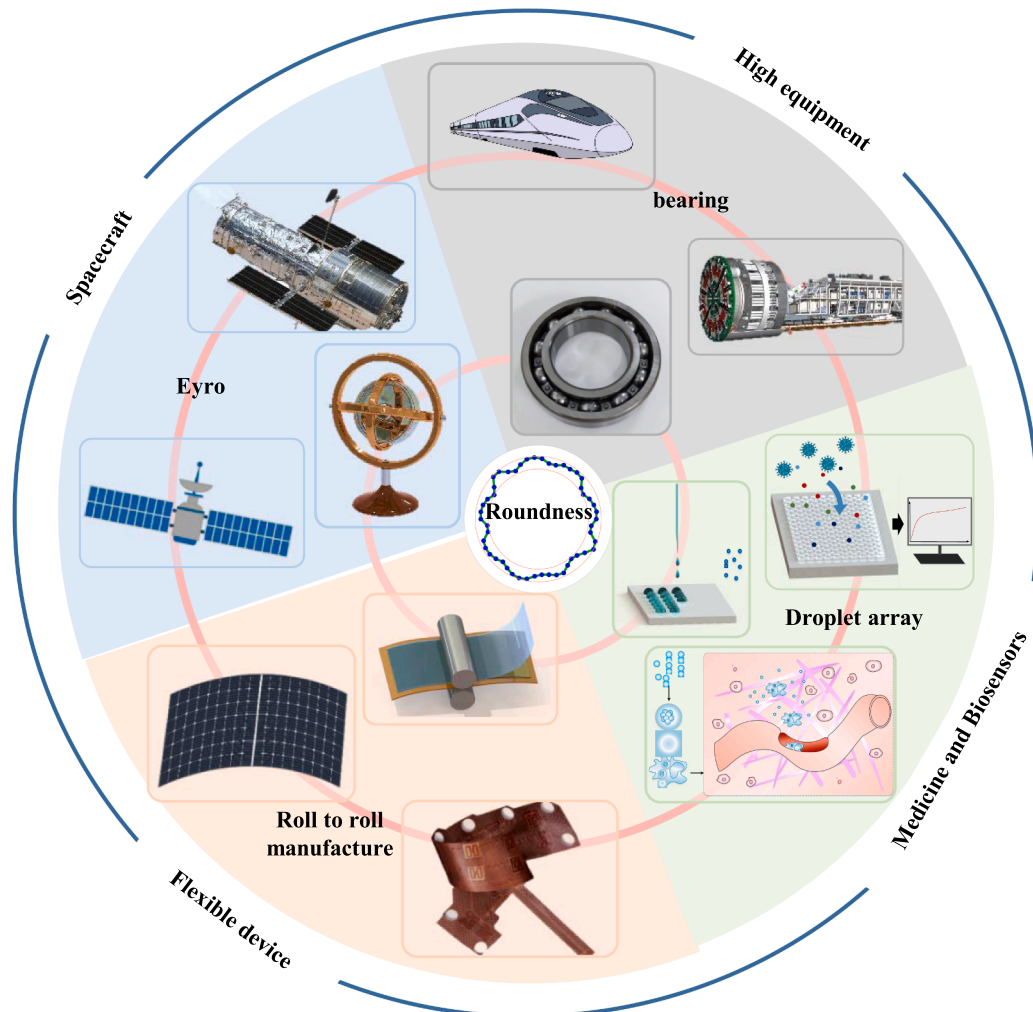


Fig. 1. Application of roundness.

Table 1
Roundness evaluation algorithm based on CG.

References	Roundness evaluation method	Description	Feature
[24]	Semi-definite programming	The problems of circularity are formulated as differentiable constrained optimization problems, and then reformulated as SDP problems.	CG-based algorithms make complex provisions and calculations to determine the iteration direction. Most of the algorithms are for profiles from a CMM that have fewer than 200 points. The calculation time will increase sharply when calculating massive point profiles.
[25]	Convex hull algorithm	Introduce the convex hull to eliminate some redundant data in polar coordinate and then calculate roundness with minimum zone lines.	
[26]	Polar Line Transformation Method	Use the idea of calculating straightness to calculate the MZC, MIC and MCC in polar coordinates.	
[27]	Intersection chord method	Calculation MZC from CMM based on the cross relationship between the chord constructed by the inner control points and the outer control points.	
[28]	Alternative exchange method	Randomly select three points and then designs an exchange criterion to update the last outer point to find the possible combinations of control points.	
[29]	Minimum zone criterion based-algorithm	Design a control point update method based on cross relationship from minimum zone criterion.	

algorithm to find the MZC. Rossi et al. [41] used an improved genetic algorithm to evaluate the MZC of a profile containing 1800 points and reduced the calculation time from 70 to 80 s to less than 9 s by optimizing the parameters. Nouira and Bourdet [42] developed a small displacement screw algorithm to satisfy the roundness calculation requirements of nano uncertainty cylindrical measuring instruments. Huang et al. [44] combined the bidirectional search of unequal probability and offset movement mechanisms to obtain the MZC, thereby greatly improving the algorithm's computational speed and stability. Li et al. [45] proposed an improved bat algorithm that combines the bat algorithm and sparrow search algorithm to calculate the MZC, thereby effectively improving the issue of the algorithm being prone to falling into local optima. Current nonlinear optimization algorithms are fast and easy to implement; however, their results are all approximate rather than an accurate optimal MZC determined by control points. If the requirement arises for high-precision calculation, the calculation time increases significantly because of the smaller iteration step size in later iterations.

A hybrid algorithm that combines the PSO algorithm and CG is proposed to achieve accurate and fast calculation of the MZC for profiles containing massive points. A new gBest selection method based on CG is added to the PSO algorithm and a minimum zone criterion that constrains the four control points is set as the termination criterion, which effectively improves the accuracy, efficiency, and stability of the MZC

Table 2
Roundness evaluation algorithm based on nonlinear optimization algorithms.

References	Roundness evaluation method	Description	Feature
[38]	New variants of PSO	Proposed five new variants of PSO altering the inertia weight, number of swarms and maximum velocity for computing the roundness error.	Their results are all approximate rather than an accurate optimal MZC determined by control points. If the requirement arises for high-precision calculation, the calculation time increases significantly because of the smaller iteration step size in later iterations.
[39]	Improved PSO method	Propose novel PSO algorithm by changing the inertia weight value and attaining its best value.	
[41]	Fast GA with five different variations	By selecting optimal GA parameters, the computation time significantly reduced when provides greater accuracy for profile with 1800 points.	
[42]	Small displacement screw roundness method	Use developed SDS method to evaluation roundness for high cylindrical measurement machine with nanometric levels of accuracy.	
[44]	Bidirectional search of unequal probability and offset movement	Combine the bidirectional search of unequal probability and offset movement mechanisms to obtain the MZC, greatly improving the algorithm's computational speed and stability.	
[45]	Improved bat algorithm	Combine the bat algorithm and sparrow search algorithm, effectively improving the issue of the algorithm being prone to falling into local optima.	

evaluation for profiles containing massive points. The performance of the algorithm was analyzed through a series of experiments. First, the accuracy of the algorithm was verified by the calculation of the MZC of four datasets from previous studies. Then, based on the constructed data obtained using a roundness measurement instrument, the trend of gBest during the iteration process and the impact of target accuracy, harmonics, and the number of points contained in the profile on the algorithm were analyzed. The results demonstrates a notable improvement in efficiency, accuracy, and stability when facing the various profiles with different number of points and harmonics. The minimum zone roundness (MZR) of datasets containing massive points from four workpieces were also calculated and the calculation time is reduced by 55 % compared to the PSO algorithm, with increased accuracy and stability. The experimental results demonstrated that the proposed algorithm greatly improved efficiency while obtaining high-precision and stable results for a profile containing massive points.

2. MZC model

The reference circle of the MZC is a set of concentric circles, in which the larger diameter is called the outer circle and the smaller diameter is called the inner circle. All points of the profile must fall within or on the annular region composed of concentric circles, and when the radius

difference between the outer circle and inner circle is minimized, the MZC is obtained. The objective function of the algorithm for the MZC calculation is usually defined as

$$F(a, b) = \min[\max(d_i) - \min(d_i)] \quad (1)$$

where d_n represents the distance from the center of the reference circle to each point of the profile. The MZR can be expressed as

$$MZR = \max(d_n) - \min(d_n) \quad (2)$$

The minimum zone criterion is used to determine whether the current reference circle is minimized, as shown in Fig. 2.

The criterion proves that MZC that meets the definition must satisfy the following three conditions [29]:

(1) All points are between or above the annular region composed of the inner circle and outer circle:

$$\min(d_n) \geq R_{inner} \text{ and } \max(d_n) \leq R_{outer} \quad (3)$$

(2) At least two points of the profile are located on the inner circle and two points of the profile are located on the outer circle.

(3) The points α_C, α_D on the inner and outer circles β_E, β_F will appear alternately with the change of angle as shown in Fig. 2. We can obtain:

$$\begin{aligned} \alpha_{\min} &= \min(\alpha_C, \alpha_D), \alpha_{\max} = \max(\alpha_C, \alpha_D) \\ \beta_{\min} &= \min(\beta_E, \beta_F), \beta_{\max} = \max(\beta_E, \beta_F) \end{aligned} \quad (4)$$

Then the relationship between the four control points can be expressed as

$$\alpha_{\min} < \beta_{\min} < \alpha_{\max} < \beta_{\max} \text{ or } \beta_{\min} < \alpha_{\min} < \beta_{\max} < \alpha_{\max} \quad (5)$$

The position of the center of the MZC is uniquely determined by the intersection point of the perpendicular bisector of CD and EF:

$$\begin{cases} y - \frac{y_C + y_D}{2} = -\frac{x_C - x_D}{y_C - y_D} \left(x - \frac{x_C + x_D}{2}\right) \\ y - \frac{y_E + y_F}{2} = -\frac{x_E - x_F}{y_E - y_F} \left(x - \frac{x_E + x_F}{2}\right) \end{cases} \quad (6)$$

3. Hybrid roundness evaluation algorithm based on CG and PSO

The flow chart of the proposed algorithm is shown in Fig. 3 and the red marker indicates the improvement of the proposed algorithm compared with the PSO algorithm.

The algorithm needs to first determine the initial value and search

range of particles, which will be introduced in detail in Sect. 3.1. Then the algorithm calculates the fitness value of each particle, updates the personal best (pBest) for each particle, and then selects the best solution from all particles to assess whether gBest should be updated. If gBest should be updated, the best solution is taken as \mathbf{gBest}_{PSO} which is same as gBest in the PSO algorithm, and a new method based on CG is added to obtain a potential solution, which is recorded as \mathbf{gBest}_{cross} . The method is detailed in Sect. 3.2. Then the better value from \mathbf{gBest}_{PSO} and \mathbf{gBest}_{cross} is selected as the final gBest. Next, the position and velocity of particles are updated according to the following update method with inertia weight:

$$\begin{cases} V_m^{k+1} = \omega \cdot V_m^k + c_1 \times rand_1 \times (pBest_m - X_m) \\ \quad + c_2 \times rand_2 \times (gBest_m - X_m) \quad m = 1, 2, \dots, M \\ X_m^{k+1} = X_m^k + V_m^{k+1} \end{cases} \quad (7)$$

where X_m and V_m represent the position and velocity of the particle and X_m are the coordinates of the potential center of the MZC. K is the number of iterations, M is the number of particles, which is set to 100, and ω is the inertia factor, which is set to 0.4. The values c_1 and c_2 are individual learning factors and social learning factors, respectively, which are all set to 2. The values $rand_1$ and $rand_2$ are random numbers in the range [0,1]. The above parameter selection was determined after some attempts based on [38]. Then the algorithm proceeds to the next iteration until the gBest meets the minimum zone criterion or reach the set maximum number of iterations.

3.1. Initial value and search range

The position selection of the initial center of the circle is based on the LSC method. It is easy to obtain the center (a_0, b_0) of LSC and least square roundness (LSR) according to the LSC method [47]. The position of initial particle (a_m, b_m) is randomly generated in a square region, with (a_0, b_0) as the center and LSR as the side length. To effectively prevent the scenario in which the optimal solution may be excluded from the initial search range, the search range is always centered on gBest, which changes dynamically with the iterations, as shown in Eq. (6) For particles that exceed the search range, the particle is randomly regenerated in the search area:

$$a_m \in \left[a_{gBest} - \frac{LSR}{2}, a_{gBest} + \frac{LSR}{2} \right], b_m \in \left[b_{gBest} - \frac{LSR}{2}, b_{gBest} + \frac{LSR}{2} \right] \quad (8)$$

3.2. New global best selection method

When the best value among all particles is better than the historical gBest, the step of updating gBest is performed. The current best value is recorded as \mathbf{gBest}_{PSO} and the proposed method generates another possible solution \mathbf{gBest}_{cross} . The distance between each point of the profile and \mathbf{gBest}_{PSO} is calculated. The nearest and second-nearest points are taken as possible control points C_k, D_k on the inner circle, and the furthest and second-furthest points are taken as possible control points E_k, F_k on the outer circle, respectively. The intersection of the vertical bisectors of the line segments $C_k D_k$ and $E_k F_k$ is solved by Eq. (6) and record as \mathbf{gBest}_{cross} . The intersection point is considered as a possible center solution and the fitness of \mathbf{gBest}_{cross} is calculated using Eq. (1). The better value from \mathbf{gBest}_{PSO} and \mathbf{gBest}_{cross} is chosen as the final gBest.

The selection method of \mathbf{gBest}_{cross} is inspired by the Voronoi diagram method based on CG. The paper [21] selected the center of the MZC from the X-type vertices, which is the intersection point of the perpendicular bisector of two segments formed by four points on the profile. It can be seen that \mathbf{gBest}_{cross} has the potential to be the optimal solution. The principle of \mathbf{gBest}_{cross} selection is substantially different from that of \mathbf{gBest}_{PSO} selection; hence, it is regarded as a mutation, which is conducive to the global search of a particle swarm and avoids falling into the local optimum. The selection of \mathbf{gBest}_{cross} also improves

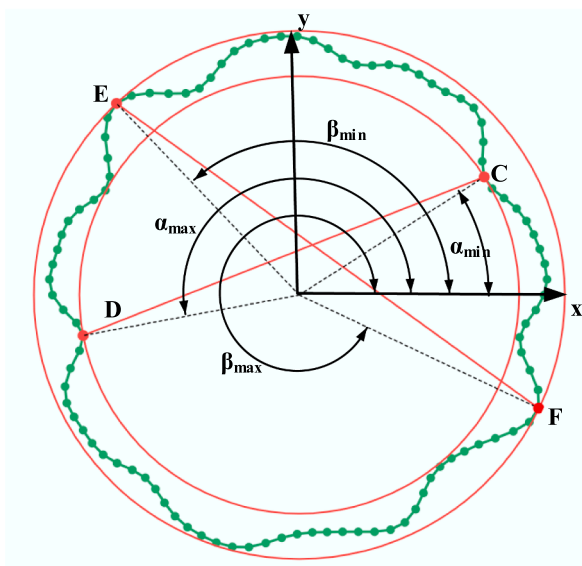


Fig. 2. Minimum zone criterion.

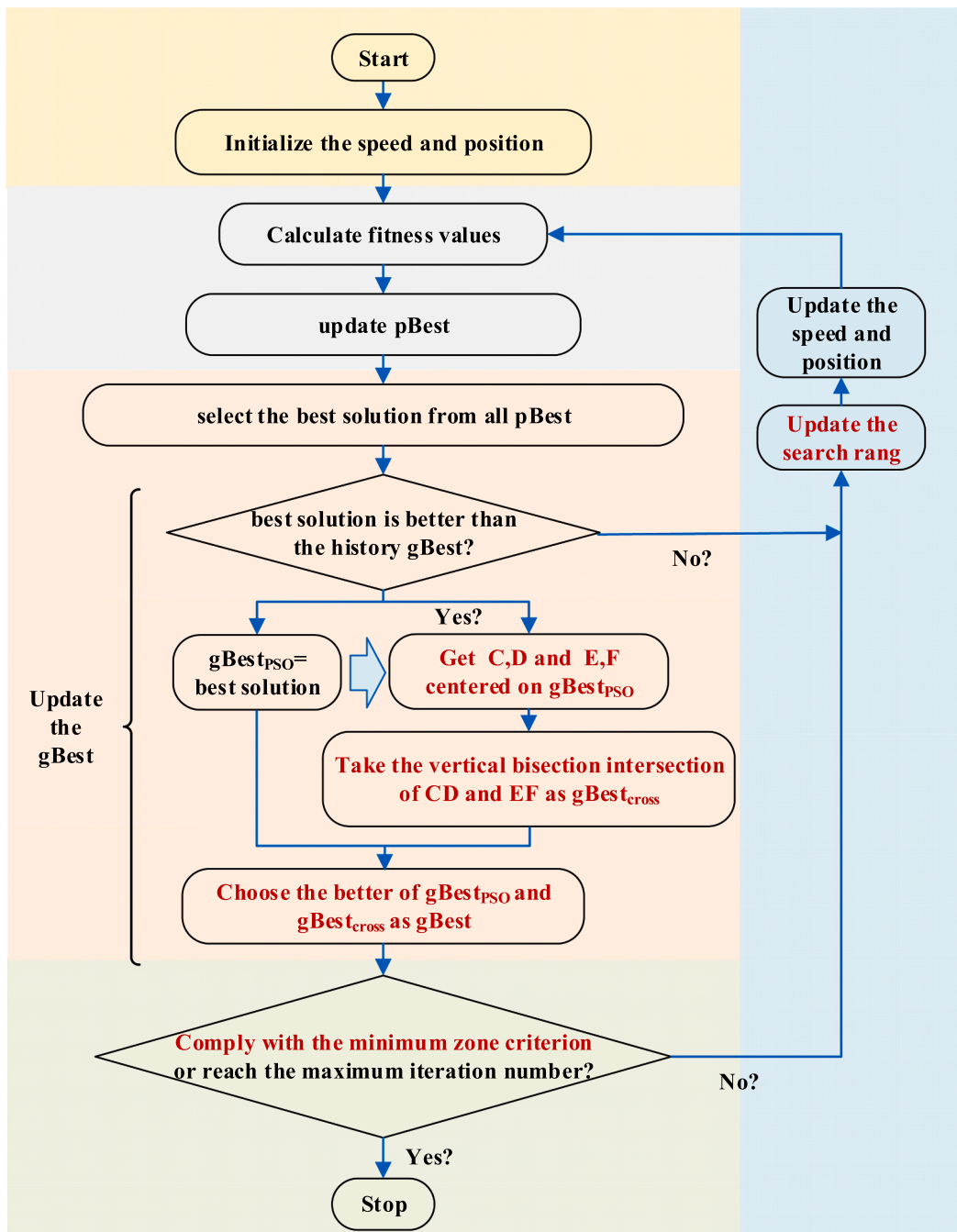


Fig. 3. Flow chart of the HCGPSO algorithm.

the convergence speed, and the control points obtained eventually conform to the partial minimum zone criterion according to the set termination criterion. Additionally, the accelerated convergence effect of the proposed algorithm is so obvious that its advantage is far greater than the increased additional calculation. These characteristics are analyzed in detail through experiments in subsequent sections.

3.3. Termination criterion

The termination criterion of the new algorithm is set to meet the minimum zone criterion or reach the set maximum number of iterations.

In each gBest update, possible control points C_k , D_k , E_k and F_k are identified during the calculation of $gBest_{cross}$ and whether the iteration stops is determined by assessing whether the four control points satisfy the minimum zone criterion. It can be seen that the possible control

points meet condition (2) of the minimum zone criterion. Then whether condition (1) is met is determined, that is, whether all points of the profile fall within the annular region controlled by points C_k , D_k , E_k and F_k . If satisfied, condition (3) is assessed, that is, whether the angle relationship of the four control points satisfies Eq. (4). If yes, the iteration terminated.

Setting the maximum number of iterations as the termination condition can prevent the search time from being too long occasionally. At this time, even if the algorithm stops without finding qualified control points, the roundness obtained has substantially met the accuracy requirements because of accelerated convergence.

4. Experiment and analysis

A series of experiments was conducted to analyze the performance of

the algorithm. In Sect. 4.1, the accuracy of the proposed algorithm is simply verified by comparing the control points and MZC results of four published datasets. In Sect. 4.2, the method of constructing points with different harmonics and different points based on the profile from roundness measurement instrument is introduced, and the trend of **gBest**_{PSO} and **gBest**_{cross} regarding iteration is analyzed to show how the new rules achieve a faster and more accurate calculation. In Sect. 4.3, the effects of the target accuracy, harmonics, and number of points contained in the profile on the performance of the algorithm are compared and analyzed. Profiles with massive points from four different workpieces are used to prove the advantages of the algorithm. The PSO algorithm is compared with the proposed algorithm, and two algorithms are run with the same parameters in the same environment.

4.1. The MZC calculation of profiles from published papers

The proposed algorithm is used to calculate MZC of dataset1-dataset4 from other literatures. The results of the control points and MZR were compared to verify whether the algorithm had a calculation error. The results are shown in Table 3.

In some studies based on the CG method [27,48,50], the results of the index of control points were provided, which is consistent with the control points obtained by the HCGPSO algorithm. The results were retained to 10⁻¹⁵ mm by the HCGPSO algorithm and the results from other algorithms were retained to 10⁻¹² mm at most [43]. The results of the control points, center, and MZR all indicate that the proposed algorithm obtained accurate results.

4.2. Profile construction and gBest iteration analysis

To make the profile closer to the actual features of the measured profile, a high-precision roundness measuring instrument was used to measure the profiles from five different workpieces to obtain dataset5-dataset9. The circularity measurement instrument utilized in our laboratory is a custom-built system with a displacement sensor boasting a measurement resolution of 1 nm, coupled with a measurement uncertainty of less than 10 nm. This precision instrument has undergone meticulous error calibration and compensation for its critical components. And employing sophisticated error separation techniques, it effectively dissects and compensates for complex instrument errors. Prior to measurement, the instrument undergoes thorough the adjustments of decenter and tilt. Datas are collected after the instrument has

been running smoothly for a period of time. Subsequently, the acquired data undergoes rigorous preprocessing, including outlier removal and filtering. Furthermore, the roundness measurement instrument has also been inspected by accredited institutions utilizing high-precision standard parts.

The measured profile was angle-displacement data containing 4000 points. The measured parts are all bearing outer rings, made of steel, with polished surfaces and diameter of 47, 45, 62, 80, and 100, respectively. Then, based on the principle of harmonic analysis, the profiles containing different harmonics and the number of points were obtained. The fluctuation trend of the profile generated by this method with different points and different harmonics tends to be consistent, which can reduce the accidental influence on performance analysis. Profile fluctuations of different frequencies are referred to as harmonics, which are represented by upr. The amplitude and phase of each upr can be determined by a fast Fourier transform. The first-order component R should be the approximate radius, which is obtained by calibrating the probe position of the roundness measuring instrument. The first-order component is considered to be eccentric and substantially less than the radius, which was set to 0. Harmonics above 500 upr are considered as noise and eliminated. The amplitude and phase from 2 upr to 500 upr for dataset5 are shown in Fig. 4(a) and 4(b).

Then the profiles containing different points and harmonics are constructed by changing the superposition parameters of the harmonic as follows:

$$p_n = R + \sum_{k=1}^K C_k \cos(k \frac{2\pi(n-1)}{N} + \varphi_k), n = 0, 1, \dots, N-1 \tag{9}$$

$$\theta_n = \frac{2\pi(n-1)}{N}, n = 0, 1, \dots, N-1 \tag{10}$$

p_n is the amplitude of the profile at angle θ_n and k is the harmonic order. Changing the size of K enables the rang of harmonics contained in the profile to be controlled. Changing the size of N enables the number of points contained in the profile to be controlled. Then the polar coordinates are transformed into rectangular coordinates to obtain the data directly used for algorithm analysis. Fig. 4(c) shows profiles containing 2–50 upr, 2–150 upr, and 2–500 upr with 1500 points. Fig. 4(d) shows profiles containing 300, 500, and 1000 points with 2–150 upr.

To prove that the introduction of **gBest**_{cross} is beneficial for obtaining a better **gBest** than the PSO algorithm, the PSO algorithm is used to

Table 3 Comparison of the results from various papers.

	x-coordinate of center	y-coordinate of center	Index of control points (inner-outer)	MZR
Dataset1				
[48]	0.00536	0.00788	63,85–36,59	957.35
[49]	0.00534671	0.00790906		957.42
[43]	0.005346707309	0.007909059150		957.419945646
[45]	0.0053467	0.0079091		957.4200
HCGPSO	0.005355464193773	0.007880734369165	63,85–36,59	957.353902655630
Dataset2				
[27]	0.0015789	−0.000910	10,72–105,45	13.518
[29]				13.51
HCGPSO	0.015789534275905	−0.000910095355967	10,72–105, 45	13.518718194177
Dataset3				
[49]	82.99094140	97.00838754		38.2304
[43]	82.990941049 445	97.008387267061		38.230943982
[50]			1,16–8,20	38.2
HCGPSO	82.990941049444501	97.008387267061352	1,16–8,20	38.230943981574
Dataset4				
[27]			12,32–15,34	8.5
[49]	0.03561497	−0.05292948		8.54
[43]	0.035614 971,221	−0.052929481201		8.537464355
HCGPSO	0.035614971220512	−0.052929481200635	12,32–15,34	8.537464354593

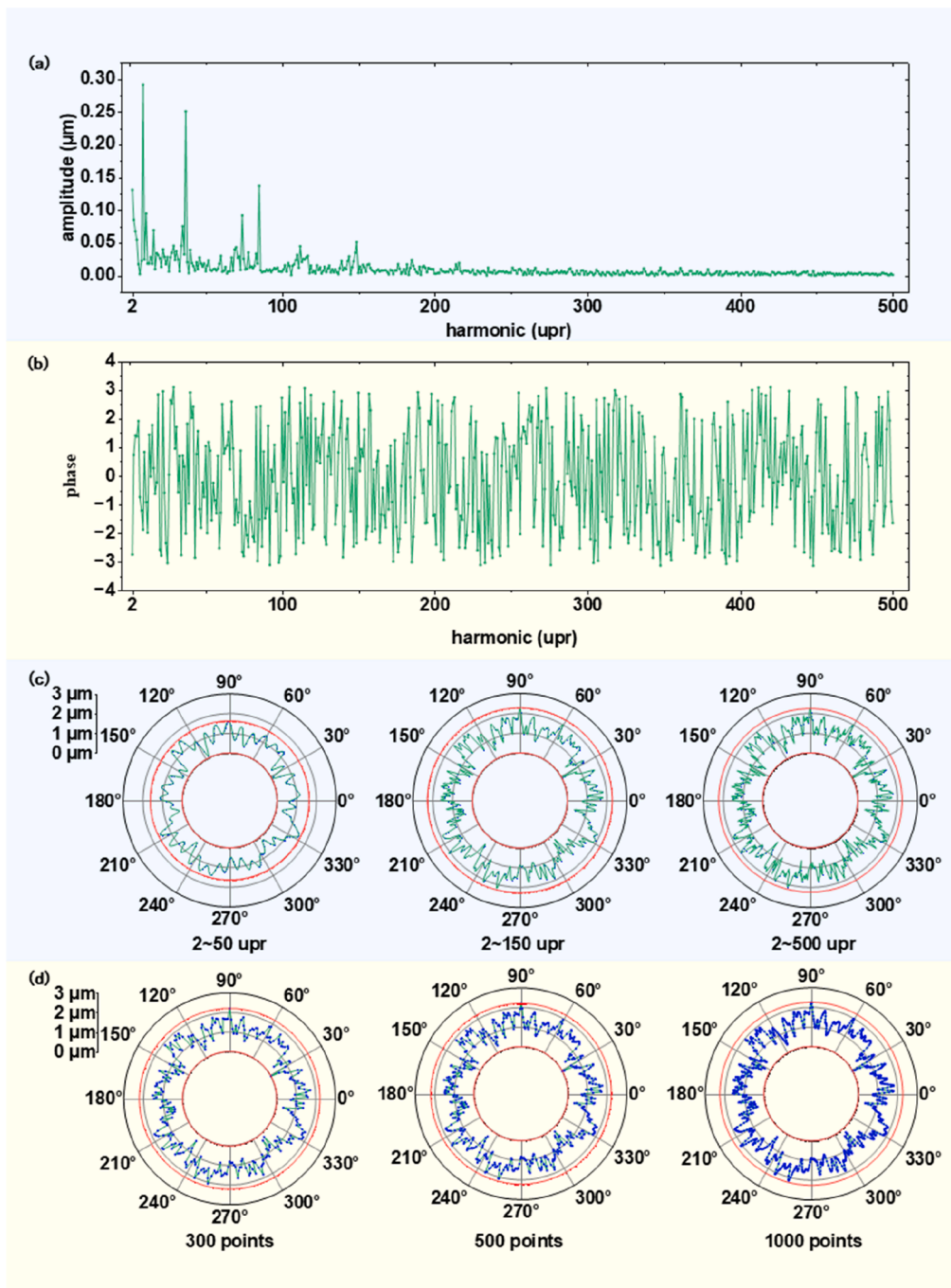


Fig. 4. Profile construction. (a) Amplitude of the profile. (b) Phase of the profile. (c) Profile with harmonic of 2–50 upr, 2–150 upr and 2–500 upr. (d) Profile with 300 points, 500 points and 1000 points.

analyze the variation and relationship between $gBest_{PSO}$ and $gBest_{cross}$. The profile containing highest harmonic of 150 upr with 1500 points was constructed based on dataset5. The maximum iteration step of the PSO algorithm was fixed at 20. After each iteration of the PSO algorithm, $gBest_{cross}$ was solved based on $gBest$, which means that $gBest_{cross}$ was only saved for analysis and no longer participated in the iteration. The calculation for one profile was repeated 1000 times. The value of $gBest$ and $gBest_{cross}$ were compared in each iteration and the number of times they appeared as the better solution were recorded. The results are shown in Fig. 5 and $gBest$ of the PSO algorithm is represented as $gBest_{PSO}$ in the figure. The horizontal axis represents the number of iterations, and the vertical axis represents the number of times that $gBest_{cross}$ and $gBest_{PSO}$ were a better value among 1000 calculations in

the corresponding step. The ratio on the bar graph is the number of times $gBest_{cross}$ was the better value divided by the total number of times of $gBest$ was updated among 1000 calculations in the corresponding step.

In the early stage (steps 1–5), the probability that $gBest_{cross}$ was the better value was less than 50%. The introduction of $gBest_{cross}$ into the proposed algorithm is regarded as a mutation, which is conducive to a full search in the global range, can prevent particles from falling into the local optimum, and can also accelerate convergence with a small probability. In the middle stage (steps 5–10), the probability that $gBest_{cross}$ was better was approximately 50%–95%, which indicates that there was a high probability that $gBest_{cross}$ was adopted as $gBest$ and effectively accelerated convergence. In the later stage (steps 11–20), the probability that $gBest_{cross}$ was better exceeded 95% until it was

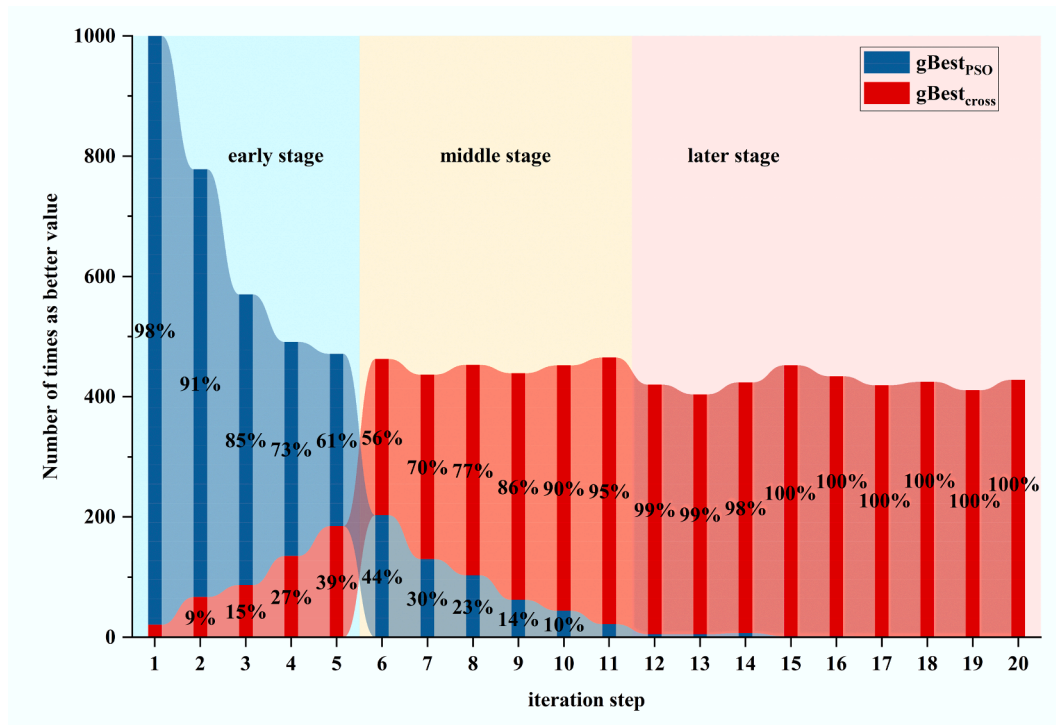


Fig. 5. Relationship between gBest_{pso} and gBest_{cross} with iterations.

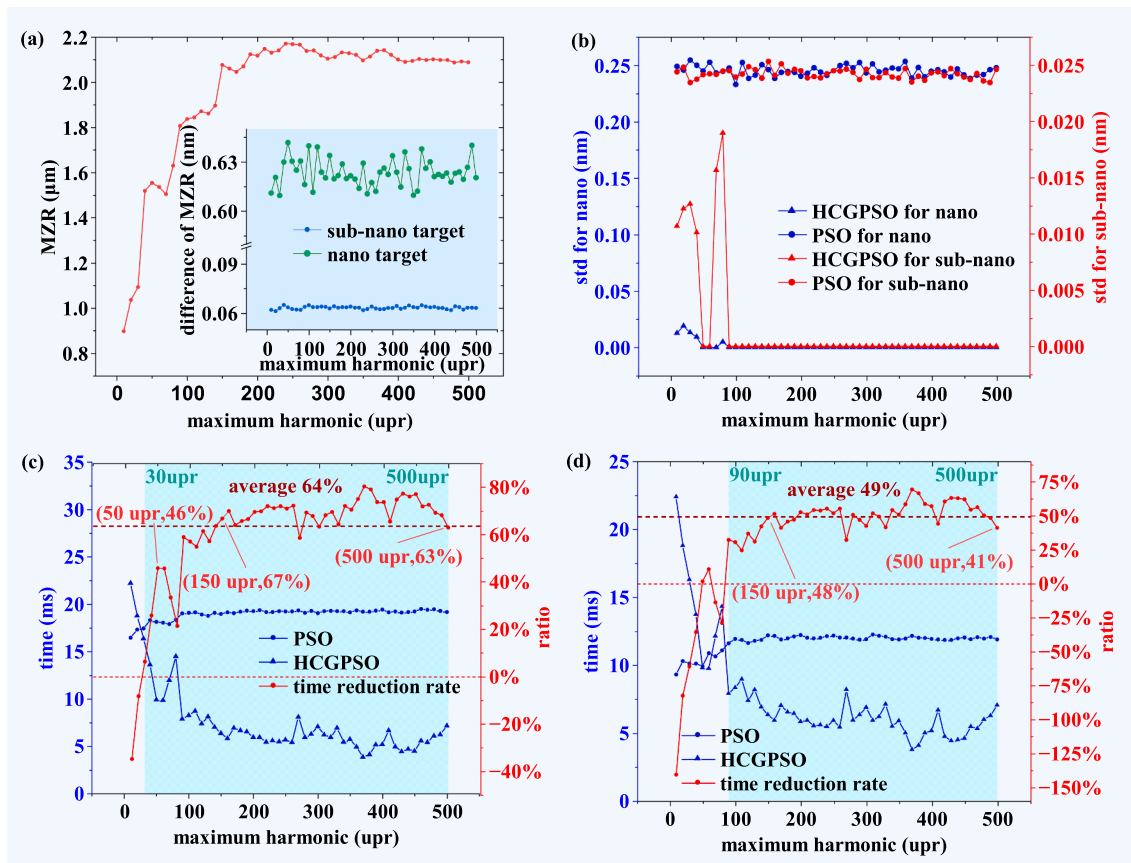


Fig. 6. Algorithm performance for profiles containing different harmonics. (a) The main image shows the ideal roundness for profiles with different harmonics. The embedded image shows the difference between the MZR obtained by the PSO algorithm and HCGPSO algorithm for different profiles with different target accuracies. (b) Standard deviation (std) of roundness solved by two algorithms for different profiles with different target accuracies. (c) Calculation time of two algorithms for different profiles with sub-nano targets. The time reduction rate is the calculation time difference between the two algorithms divided by the calculation time taken by the PSO algorithm. (d) Calculation time of two algorithms for different profiles with nano targets.

close to 100 %. The introduction of $gBest_{cross}$ almost accelerated the iteration of the algorithm, and control points that satisfied the minimum zone criterion were obtained quickly based on the termination criterion. Simultaneously, it can be seen that $gBest_{cross}$ depended, to a certain extent, on $gBest_{ps0}$. This means that after $gBest_{ps0}$ was optimized to the target accuracy, the calculation of $gBest_{cross}$ was invalid, even if $gBest_{cross}$ achieved higher accuracy. Therefore, the target accuracies that affected the advantages of the HCGPSO and PSO algorithm differed. The experiments in next section will also prove this conclusion.

The analysis in this section indicates that the new rule obtained a better $gBest$ than the PSO algorithm, which effectively improved computational efficiency.

4.3. Analysis of the impact of profiles on algorithm performance

In practical applications, the uncertainty of some high-precision roundness measurement equipment has reached the sub-nano [39]. The sub-nano and nano were set as target accuracies in subsequent analysis, and the termination criterion of the PSO algorithm was adjusted according to the target accuracy. The proposed algorithm was iterated for a sufficient time until it obtained control points that satisfied the minimum zone criterion. This MZR value is considered as the theoretical optimal MZR. The PSO algorithm was set to stop when $gBest$ was better than $MZR + 0.1 \text{ nm}/1 \text{ nm}$, whereas the termination criterion of the HCGPSO algorithm was still as described in Sect. 3.3. The calculation was repeated 1000 times for each profile and the average value of roundness, standard deviation, and average calculation time were

recorded for each profile. After our test, the results displayed by the algorithm in 1000 runs have stabilized. The initial particle positions for two algorithms remained consistent in each calculation.

Then profiles that contained the highest harmonic of 10–500 upr with 1500 points were constructed based on dataset5 to analyze the impact of different harmonics contained in profiles on the algorithm performance for sub-nano and nano target accuracy. The results are shown in Fig. 6.

For sub-nano target accuracy, the calculation time of the HCGPSO algorithm reduced by 64 % on average compared with the PSO algorithm for profiles whose highest harmonic was greater than 30upr. The calculation time of profiles with the highest harmonics of 50 upr, 150 upr and 500 upr is reduced by 46 %, 67 % and 63 %, respectively. The average roundness difference between nano and sub nano precision algorithms is about 0.6 nm and 0.06 nm, respectively. The accuracy of propose algorithm is significantly better than the PSO algorithm. The standard deviation of the proposed algorithm was better than those of the PSO algorithm and the standard deviation of the proposed algorithm was equal to 0 for the profile with the highest harmonic greater than 90 upr. For nano target accuracy, the calculation time reduced by 49 % on average compared with that of the PSO algorithm for profiles whose highest harmonic was greater than 90 upr. The calculation time of profiles with highest harmonic of 150 upr and 500 upr reduced by 48 % and 41 %, respectively. The accuracy and stability of the calculation results were also better than those of the PSO algorithm. The results show that the HCGPSO algorithm had a greater advantage when sub-nano was used as the target accuracy than when nano was used. For

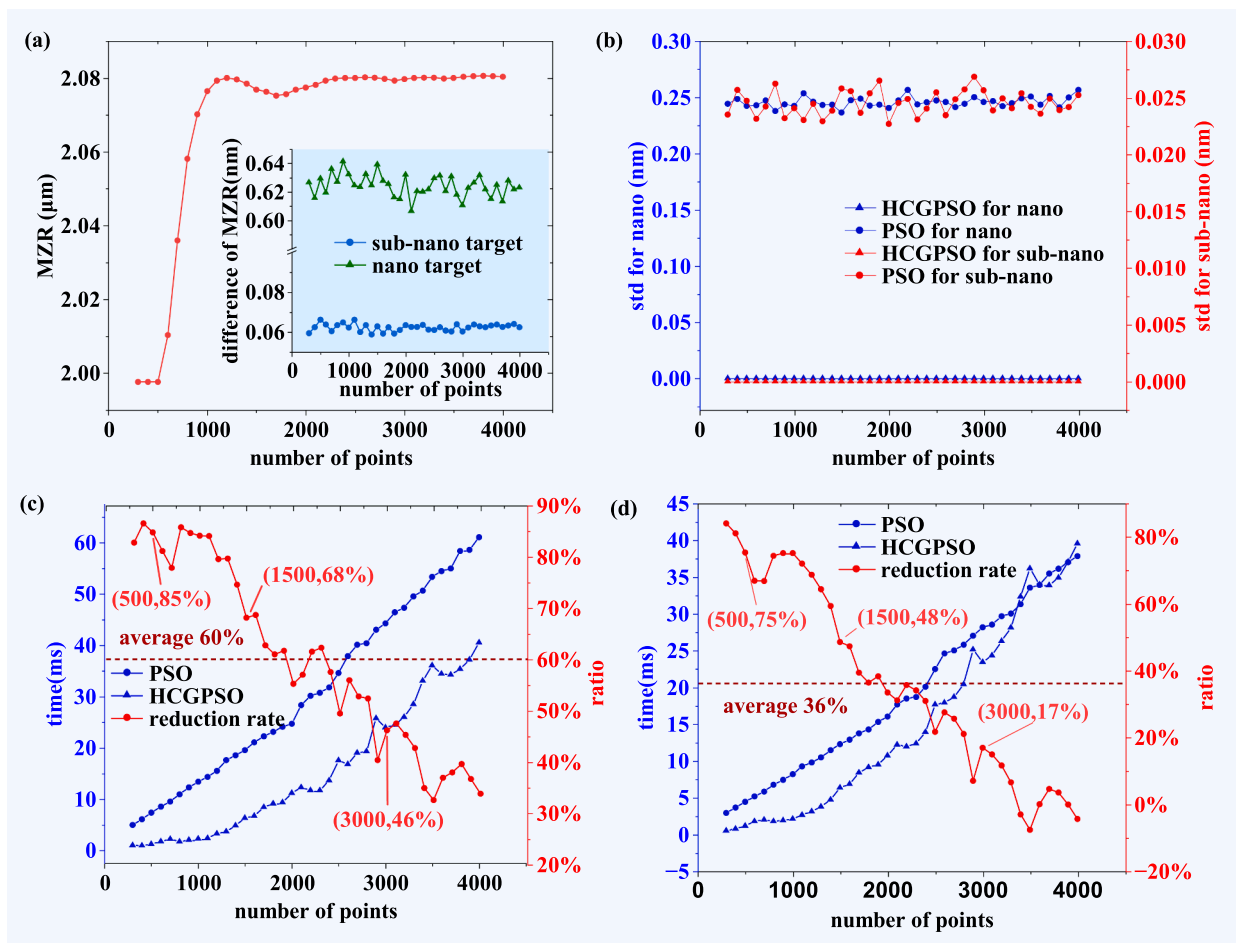


Fig. 7. Algorithm performance for profiles containing different numbers of points. (a) The main image shows the ideal roundness. The embedded image shows the MZR difference of the HCGPSO and PSO algorithms. (b) Standard deviation of roundness for profiles containing different numbers of points. (c) Calculation time for profiles with sub-nano targets. (d) Calculation time for profiles with nano targets.

some profiles that only contained extremely low harmonics, the performance advantages of the proposed algorithm were also weak. This implies that the gentle fluctuation of the profile led to little change in the selection of control points with the change of $gBest_{PSO}$.

To analyze the impact of the profile containing different number of points on the performance of HCGPSO algorithm, profiles of 300–4000 points with the highest harmonic of 150 upr were constructed. The results are shown Fig. 7.

For sub-nanometer target accuracy, the calculation time of the HCGPSO algorithm for profiles with different numbers of points reduced by 60 % on average compared with that of the PSO algorithm. The calculation time of profiles with 500, 1500, and 3000 points reduced by 85 %, 68 %, and 46 %. For nano target accuracy, the calculation time of the proposed algorithm reduced by 36 % on average. The calculation time of profile with 500, 1500, 3000 points reduced by 75 %, 48 %, and 17 % respectively. The proposed algorithm also significant improved in accuracy and stability compared with the PSO algorithm. The analysis also shows that the advantage of the proposed algorithm in terms of efficiency gradually reduced as the number of profile points increased.

Finally, to prove the feasibility of the proposed algorithm for the MZC calculation of the profile with massive points, the dataset6-dataset9 were obtained from four workpieces with diameter of 45, 62, 80, and 100 using the roundness measuring instrument, as shown in

Fig. 8.

Profiles contained the highest harmonic of 500 upr with 4000 points were constructed. Taking sub-nanometer as target accuracy, calculation time and standard deviation are compared and the results are shown in Table 4.

The calculation time of the HCGPSO algorithm for dataset6-dataset9 reduced by 54 %, 65 %, 39 %, and 64 %, with an average reduction of 55 %. The MZR of the proposed algorithm was still approximately 0.064 nm smaller than that of the PSO algorithm. The standard deviation was also better than that of the PSO algorithm, and three of MZR standard

Table 4

Comparison of the results of dataset6-dataset9.

		Dataset6	Dataset7	Dataset8	Dataset9
MZR (μm)		1.2106	4.0190	4.0949	0.9724
time (ms)	HCGPSO	19.12	22.25	40.54	17.02
	PSO	41.80	62.96	66.11	46.82
Difference of MZR (nm)		0.0639	0.0637	0.0650	0.0650
Standard deviation (nm)	HCGPSO	0.0000	0.0000	0.0000	0.0000
	PSO	0.0245	0.0245	0.0237	0.0243

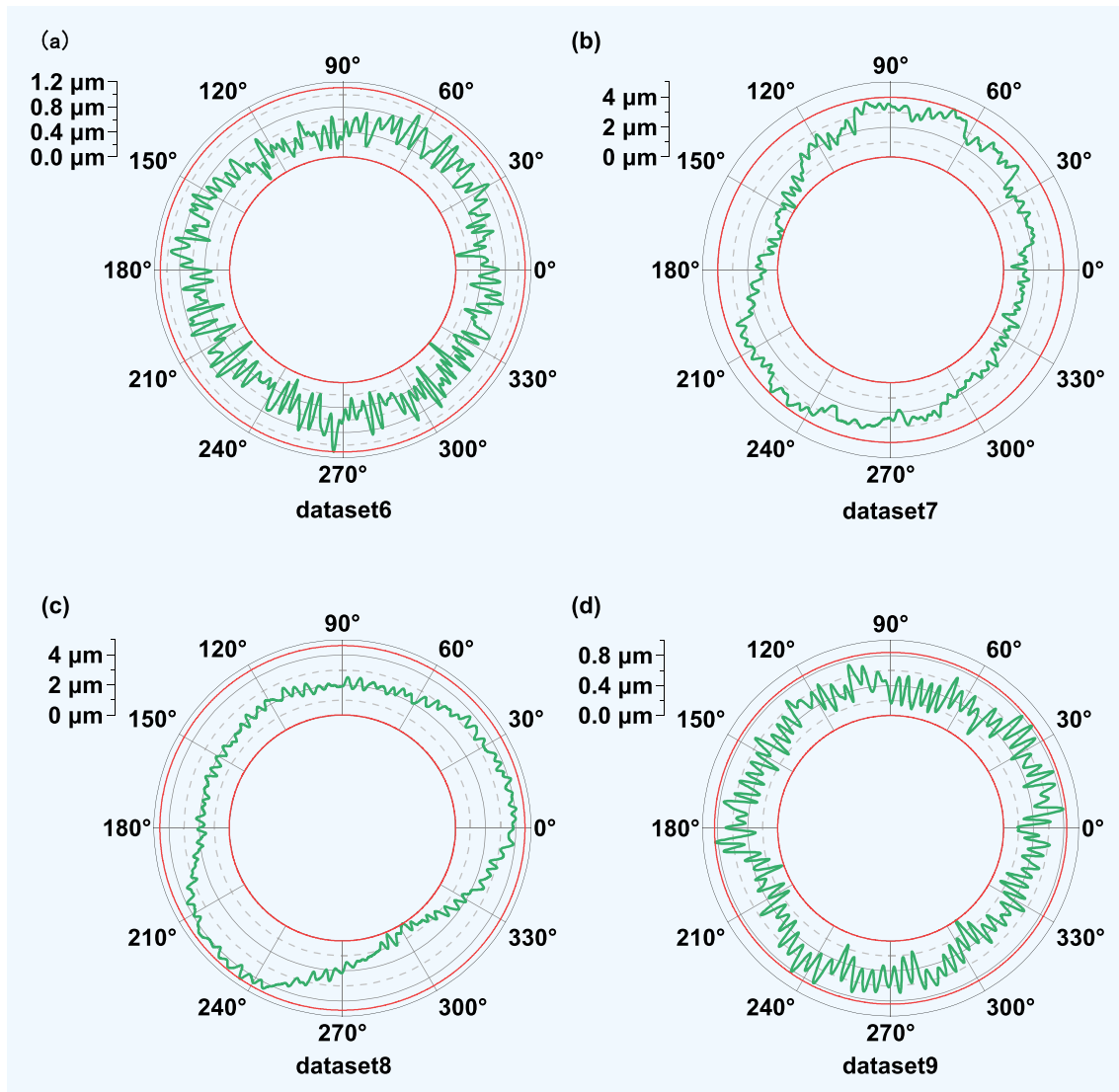


Fig. 8. profile from different workpieces. (a) dataset6. (b) dataset7. (c) dataset8. (d) dataset9.

deviation were 0.

In this section, we give the calculation time, calculation accuracy, and standard deviation of the PSO algorithm and the HCGPSO algorithm for MZC evaluation with different target accuracy and the profiles containing different numbers of points and harmonics. For nanometer and sub-nanometer target accuracy, our proposed algorithm exhibits a superior computational efficiency at sub-nano level compared to the nano. This demonstrates that the new rules designed by the algorithm can function more effectively when facing higher precision calculation requirements. In the evaluation of profiles containing 10–500 upr and 300–4000 points, the efficiency of the HCGPSO algorithm is improved by over 30 % at the sub-nano target. The standard deviation of the results also indicates that the stability of the HCGPSO algorithm is better than that of the PSO algorithm. In profiles containing 4000 points from four different workpieces, the algorithm's average efficiency increases by 55 %. Moreover, the accuracy and standard deviation of the HCGPSO algorithm are significantly better than those of the PSO algorithm.

The analysis above demonstrates that the HCGPSO algorithm exhibits high precision and remarkable solution stability. Notably, its standard deviations are consistently smaller than those of the PSO algorithm, and in many cases, approach 0. Although we employed a relatively broad initial particle position range to ensure the accuracy of the algorithm, the algorithm still has strong repeatability, which is an advantage of using the minimum zone criterion as the iteration termination criterion. In terms of computational efficiency, the HCGPSO algorithm has made significant advancements over the PSO algorithm. Its combination with the crossover criterion during the iterative process of the global best value determines that the algorithm can greatly improve in terms of computational efficiency, while also laying the foundation for the modification of the iterative stopping condition. This is attributed to its integration with the minimum zone criterion throughout the iterative process for gBest values, contributing substantially to enhanced computational efficiency while laying the groundwork for iteration termination condition refinements. Above all, the HCGPSO algorithm demonstrates a notable improvement in efficiency, accuracy, and stability when facing the requirements of MZR calculations for high-precision profiles with a large number of points. The algorithm is capable of meeting the practical needs for evaluating the MZR of different profiles.

In addition to the aforementioned advantages, we have also identified some other characteristics of the algorithm that necessitate discussion in this context. For some profiles that only contain extremely low harmonics, the performance advantages of the proposed algorithm are also weak. It is speculated the gentle fluctuation of the profile leads to little change in the selection of control points with the change of $gBest_{PSO}$. As a result, $gBest_{cross}$ cannot effectively accelerate convergence and invalid calculation is introduced. Furthermore, we consider this to be a normal occurrence since different profiles exhibit varying degrees of complexity, which can often hinder the distinction of the optimal profile value from local optima. Even conventional PSO algorithms exhibit significantly different computation times when dealing with these profiles, and the new algorithm exhibits similar characteristics.

5. Conclusions and future works

Faced with requirements for the high-precision and efficient roundness evaluation of MZC for profile containing massive points, the algorithm based on CG takes a long time, and the nonlinear optimization algorithm cannot obtain accurate results. The HCGPSO algorithm is proposed to improve efficiency while obtaining high-precision results. A gBest search method based on CG was added and a termination criterion based on the minimum zone criterion was set. The new method was conducive to the full search of a particle swarm in the global range and avoided falling into the local optimum in the early stage of iteration. It effectively accelerated the search for the global best until control points

that met the minimum zone criterion were found.

A series of experiments were conducted to analyze the performance of the algorithm. The calculation of the MZC for four published datasets indicated that the HCGPSO algorithm correctly identified MZC and the results were displayed to 10^{-15} mm. The change of gBest during the iteration was shown to prove that new rules effectively accelerated convergence and accurately obtained the control points. Then the impact of target accuracy, harmonics, and number of points contained in the profile on the HCGPSO algorithm were analyzed. The HCGPSO algorithm had stronger advantages for higher calculation accuracy requirements. With sub-nanometer target evaluation precision, the efficiency of HCGPSO improved by an average of 64 % for profiles containing the highest harmonics from 30 upr to 500 upr with 1500 points. An average efficiency improvement of 60 % was observed for profiles with 300 to 4000 points at 150 upr. For profiles with 4000 points at 500 upr from four workpieces, the calculation time is reduced by 55 % on average compared to the PSO algorithm, with increased accuracy and stability. The proposed algorithm effectively achieved a high-precision and high-efficiency MZC calculation for profile containing massive points.

The proposed method can also be used in other nonlinear optimization algorithms, which provides a good idea for calculating the MZC. Additionally, the improvement of the algorithm is based on the conventional PSO algorithm and there is still room for improvement, such as the adjustment of range of the initial value, inertia weight, learning factor, and particle velocity update method; hence its performance will be further improved in future work. The HCGPSO algorithm has the potential for combining the particle swarm optimization algorithm with the triangle criterion and line criterion to enhance the algorithm's performance in the evaluation of MIC and MCC. In addition, profile containing more points will be obtained with the advancement of measurement technology in the future. The performance of the new algorithm will be further optimized in the future.

CRedit authorship contribution statement

Xuelong Bai: Conceptualization, Methodology, Software, Writing – original draft. **Wei Wang:** Supervision, Writing – review & editing. **Wenhao li:** Project administration. **Zhaowu Liu:** Funding acquisition. **Shuo Yu:** Resources. **Yu Bai:** Investigation. **Guoxue Chen:** Investigation.

Declaration of Competing Interest

The authors declare that they have no known competing financial interests or personal relationships that could have appeared to influence the work reported in this paper.

Data availability

Data will be made available on request.

Acknowledgments

Thank you to Professor Li Wenhao and Professor Wei Wang of Changchun Institute of Optics, Fine Mechanics and Physics, Chinese Academy of Sciences, for their help and support. This work was partially funded by the Strategic Priority Research Program of the Chinese Academy of Sciences grant XDC04030100, Changchun Science & Technology Development Program Project in China grant 21SH07, Chinese Academy of Sciences Youth Innovation Promotion Association grant 2021220, and National Natural Science Foundation of China grant U21A20509.

References

- [1] P. Toren, M. Smolka, A. Haase, U. Palfinger, D. Nees, et al., High-throughput roll-to-roll production of polymer biochips for multiplexed DNA detection in point-of-care diagnostics, *Lab Chip* 20 (2020) 4106–4117.
- [2] L. Kong, S. Cao, J.-H. Chin, Y. Si, F. Miao, et al., Vibration suppression of drilling tool system during deep-hole drilling process using independence mode space control, *Int. J. Mach. Tools Manuf.* 151 (2020) 103525.
- [3] P. Cui, L. Du, X. Zhou, J. Li, Y. Li, et al., Harmonic vibration control of MSCMG based on multisynchronous rotating frame transformation, *IEEE Trans. Ind. Electron.* 69 (2022) 1717–1727.
- [4] M. Tsutsumi, S. Tone, N. Kato, R. Sato, Enhancement of geometric accuracy of five-axis machining centers based on identification and compensation of geometric deviations, *Int. J. Mach. Tools Manuf.* 68 (2013) 11–20.
- [5] R. Viitala, T. Widmaier, P. Kuosmanen, Subcritical vibrations of a large flexible rotor efficiently reduced by modifying the bearing inner ring roundness profile, *Mech. Syst. Sig. Process.* 110 (2018) 42–58.
- [6] F. Zhang, Z. Yang, Development of and perspective on high-performance nanostructured bainitic bearing steel, *Engineering* 5 (2019) 319–328.
- [7] T.-Y. Chien, R. Marín-Benavides, S. Belkin, J.-Y. Cheng, Rapid printing of a bacterial array for a solid-phase assay (BacSPA) of heavy metal ions, *Sens. Actuators, B Chemical* 359 (2022) 131540.
- [8] Y. Liu, N. Tottori, T. Nisisako, Microfluidic synthesis of highly spherical calcium alginate hydrogels based on external gelation using an emulsion reactant. “Sens, Actuators, b” 283 (2019) 802–809.
- [9] O. Jusko, M. Neugebauer, H. Reimann, W. Sabuga, T.J.P. Priruenrom, Informative bulletin Of The interamerican metrology system—OAS. 2009. Dimensional calibration techniques for pressure balances to be used in the new determination of the Boltzmann constant, PTB, Informative Bulletin Of The Interamerican Metrology System-OAS (2009).
- [10] S. Cappa, D. Reynaerts, F. Al-Bender, A sub-nanometre spindle error motion separation technique, *Precis. Eng.* 38 (2014) 458–471.
- [11] G. Zongchao, T. Zhen, J. Xiangqian, Review of geometric error measurement and compensation techniques of ultra-precision machine tools, *Light Advanced Manufacturing* 2 (2021) 211–227.
- [12] E. Marsh, J. Couey, R. Vallance, Nanometer-level comparison of three spindle error motion separation techniques, *J. Manuf. Sci. Eng.* 128 (2005) 180–187.
- [13] S.C. Toguem Tagne, A. Vissiere, M. Damak, C. Mehdi-Souzani, N. Anwer, et al., An advanced Fourier-based separation method for spindle error motion identification, *Precis. Eng.* 74 (2022) 334–346.
- [14] A. Vissiere, H. Noura, M. Damak, O. Gibrar, J.M. David, Concept and architecture of a new apparatus for cylindrical form measurement with a nanometric level of accuracy, *Meas. Sci. Technol.* 23 (2012) 094014.
- [15] V. Alain, N. Hichem, D. Mohamed, G. Olivier, Implementation of capacitive probes for ultra-high precision machine for cylindricity measurement with nanometric level of accuracy, *Int. J. Precis. Eng. Manuf.* 16 (2015) 883–893.
- [16] Z. Tan, X. Jiang, Y. Mao, X. Long, H. Luo, Ultra-smooth surface with 0.4 Å roughness on fused silica, *Ceram. Int.* 49 (2023) 7245–7251.
- [17] Y. Dong, P.-C. Hu, H. Fu, H. Yang, R. Yang, et al., Long range dynamic displacement: Precision PGC with sub-nanometer resolution in an LWSM interferometer, *Photonics Res.* 10 (2022) 59–67.
- [18] E.S. Gadelmawla, Simple and efficient algorithms for roundness evaluation from the coordinate measurement data, *Measurement* 43 (2010) 223–235.
- [19] F. Liu, Y. Cao, T. Li, L. Ren, J. Zhi, et al., An Iterative Minimum Zone Algorithm for assessing cylindricity deviation, *Measurement* 213 (2023) 112738.
- [20] J. Huang, R. Yang, H. Ge, J. Tan, An effective determination of the minimum circumscribed circle and maximum inscribed circle using the subzone division approach, *Meas. Sci. Technol.* 32 (2021) 075014.
- [21] J. Huang, An exact solution for the roundness evaluation problems, *Precis. Eng.* 23 (1999) 2–8.
- [22] J. Huang, E.A. Lehtihet, Contribution to the minimax evaluation of circularity error, *Int. J. Prod. Res.* 39 (2001) 3813–3826.
- [23] L. Vandenberghe, S. Boyd, Semidefinite programming, *SIAM Rev.* 38 (1996) 49–95.
- [24] Y. Ding, L. Zhu, H. Ding, A unified approach for circularity and spatial straightness evaluation using semi-definite programming, *Int. J. Mach. Tools Manuf.* 47 (2007) 1646–1650.
- [25] L. Xiuming, S. Zhaoyao, Application of convex hull in the assessment of roundness error, *Int. J. Mach. Tools Manuf.* 48 (2008) 711–714.
- [26] R. Calvo, E. Gomez, Accurate Evaluation of Functional Roundness from Point coordinates, *Measurement* 73 (2015) 211–225.
- [27] L. Fei, X. Guanghua, L. Lin, Z. Qing, L. Dan, Intersecting chord method for minimum zone evaluation of roundness deviation using Cartesian coordinate data, *Precis. Eng.* 42 (2015) 242–252.
- [28] A. Khilil, Z. Shi, A. Umar, B. Ma, Improved algorithm for minimum zone of roundness error evaluation using alternating exchange approach, *Meas. Sci. Technol.* 33 (2022) 045003.
- [29] M. Zhuo, J. Geng, C. Zhong, K. Xia, New accurate algorithms of circularity evaluation, *Meas. Sci. Technol.* 34 (2023) 025019.
- [30] H. Mohammadzadeh, F.S. Gharehchopogh, A multi-agent system based for solving high-dimensional optimization problems: A case study on email spam detection, *Int. J. Commun. Syst.* 34 (2021) e4670.
- [31] F.S. Gharehchopogh, B. Abdollahzadeh, An efficient harris hawk optimization algorithm for solving the travelling salesman problem, *Clust. Comput.* 25 (2022) 1981–2005.
- [32] S.T. Shishavan, F.S. Gharehchopogh, An improved cuckoo search optimization algorithm with genetic algorithm for community detection in complex networks, *Multimed. Tools Appl.* 81 (2022) 25205–25231.
- [33] F.S. Gharehchopogh, An improved harris hawks optimization algorithm with multi-strategy for community detection in social network, *J. Bionic Eng.* 20 (2023) 1175–1197.
- [34] F.S. Gharehchopogh, Quantum-inspired metaheuristic algorithms: comprehensive survey and classification, *Artif. Intell. Rev.* 56 (2023) 5479–5543.
- [35] F.S. Gharehchopogh, T. Ibricci, An improved African vultures optimization algorithm using different fitness functions for multi-level thresholding image segmentation, *Multimed. Tools Appl.* (2023).
- [36] F.S. Gharehchopogh, A.A. Khargoush, A chaotic-based interactive autodidactic school algorithm for data clustering problems and its application on COVID-19 disease detection, *Symmetry* 15 (2023).
- [37] F.S. Gharehchopogh, A. Ucan, T. Ibricci, B. Arasteh, G. Isik, Slime mould algorithm: A comprehensive survey of its variants and applications, *Arch. Comput. Methods Eng.* 30 (2023) 2683–2723.
- [38] T.-H. Sun, Applying particle swarm optimization algorithm to roundness measurement, *Expert Syst Appl.* 36 (2009) 3428–3438.
- [39] C.-l. Du, C.-x. Luo, H. Z-t, Y.-s. Zhu, Applying particle swarm optimization algorithm to roundness error evaluation based on minimum zone circle, *Measurement* 52 (2014) 12–21.
- [40] X. Wen, Q. Xia, Y. Zhao, An effective genetic algorithm for circularity error unified evaluation, *Int. J. Mach. Tools Manuf.* 46 (2006) 1770–1777.
- [41] A. Rossi, M. Antonetti, M. Barloscio, M. Lanzetta, Fast genetic algorithm for roundness evaluation by the minimum zone tolerance (MZT) method, *Measurement* 44 (2011) 1243–1252.
- [42] H. Noura, P. Bourdet, Evaluation of roundness error using a new method based on a small displacement screw, *Meas. Sci. Technol.* 25 (2014) 044012.
- [43] Y. Zheng, A simple unified branch-and-bound algorithm for minimum zone circularity and sphericity errors, *Meas. Sci. Technol.* 31 (2020) 045005.
- [44] J. Huang, X. Chao, L. Jiang, R. Yang, J. Tan, Improved evaluation of minimum zone roundness by integrating bidirectional search of unequal probability and offset mechanisms, *Meas. Sci. Technol.* 30 (2019) 125014.
- [45] G. Li, Y. Xu, C. Chang, S. Wang, Q. Zhang, et al., Improved bat algorithm for roundness error evaluation problem, *Math. Biosci. Eng.* 19 (2022) 9388–9411.
- [46] A. Rossi, M. Lanzetta, Minimal exhaustive search heuristics (MESH) of point clouds for form tolerances: The minimum zone roundness, *Precis. Eng.* 43 (2016) 154–163.
- [47] C. Zhi-min, W. Yun, H. Jian, Roundness deviation evaluation method based on statistical analysis of local least square circles, *Meas. Sci. Technol.* 28 (2017) 105017.
- [48] J. Huang, A new strategy for circularity problems, *Precis. Eng.* 25 (2001) 301–308.
- [49] D.S. Srinivasu, N. Venkaiah, Minimum zone evaluation of roundness using hybrid global search approach, *Int. J. Adv. Manuf. Technol.* 92 (2017) 2743–2754.
- [50] X. Li, Z. Shi, The relationship between the minimum zone circle and the maximum inscribed circle and the minimum circumscribed circle, *Precis. Eng.* 33 (2009) 284–290.